Spatial aspects of urban air quality management: Estimating the impact of micro-scale urban form on pollution dispersion

Joanna Badach [a,*], Wojciech Wojnowski [b,1], Jacek Gębicki [c]

[a] Department of Urban Architecture and Waterscapes, Faculty of Architecture, Gdańsk University of Technology, 11/12 Narutowicza Street, 80-233 Gdańsk, Poland
[b] Department of Analytical Chemistry, Faculty of Chemistry, Gdańsk University of Technology, 11/12 Narutowicza Street, 80-233 Gdańsk, Poland
[c] Department of Process Engineering and Chemical Technology, Faculty of Chemistry, Gdańsk University of Technology, 11/12 Narutowicza Street, 80-233 Gdańsk, Poland

ARTICLE INFO

ABSTRACT

Urban planning and design solutions affect urban ventilation conditions, thus mitigating the effects of atmospheric pollution. However, these findings are not being implemented in the planning practice to a sufficient extent, partly due to the lack of specific guidelines. Moreover, many urban air quality monitoring (AQM) sites have low represnentativeness and thus do not provide comprehensive data for effective urban air pollution control with respect to the urban spatial policy. An integrated assessment method based on modelling, simulation, and geospatial data processing tools was used to investigate the impact of micro-scale urban form on the local ventilation conditions and pollution dispersion. The proposed approach combined computational fluid dynamics (CFD) and geographic information system (GIS) tools, and particularly the newly developed Residence Time Index (RTI) - a single CFD-derived parameter quantifying the capabilities of the micro-scale built environment to retain PM10 pollution. Urban segments around monitoring sites in three Polish cities (Gdańsk, Warsaw, and Poznań), characterised by relatively low density and varied urban form typologies, were investigated. The results indicate that in these conditions the following features of the urban form have the strongest correlation with the RTI: plan area density (λ_P), gross floor area ratio (λ_{GFA}), and occlusivity (O_c), making them useful indicators for urban air quality management. On the other hand, PM10 data from the AQM sites are rather poorly linked with urban form indicators, which suggests that in complex urban scenarios a higher spatial resolution of air quality data is required for shaping the spatial policy. The implications from this analysis are useful for the urban planning practice. The developed approach may be also a valuable decision support tool for the assessment of the spatial representativeness of AQM sites.

1. Introduction

According to the experts at the World Health Organization (2022), over 4 million cases of premature deaths every year are the result of the exposure to outdoor air pollution. This issue may be partly tackled by means of appropriate urban planning solutions as there is a strong link between the urban form, wind environment, and air pollution (Yang et al., 2020). Although the understanding of these interactions is still insufficient (da Silva, Reis, Santos, Goulart, & de Alvarez, 2022; Yuan, Ng, & Norford, 2014), this field of research has been developing very rapidly in the recent years. A wide range of studies have been conducted to simulate how air flow and pollution dispersion is affected by the configuration and features of the urban form. Up-to-date computational fluid dynamics (CFD) simulations are considered most suitable for this purpose, allowing to accurately account for the effect of building morphologies (da Silva, Reis, Santos, Goulart, & Engel de Alvarez, 2021; Johansson & Yahia, 2020; Lauriks et al., 2021; Qin, Lin, Lau, & Song, 2020; Zhang et al., 2021). However, despite the recent advancements, CFD simulations are still very complex, computationally expensive, and require expert knowledge (Mirzaei, 2021).

Due to the high complexity and considerable computational costs of the CFD studies, many of them are restricted to the urban micro-scale (the scale of separated street canyons, building complexes or urban blocks) (Acero, Koh, Ruefenacht, & Norford, 2021; Azizi & Javanmardi, 2017; da Silva et al., 2022; Du, Blocken, & Pirker, 2020; Kaseb, Hafezi, Tahbaz, & Delfani, 2020; Lauriks et al., 2021; Qin et al., 2020; Ramponi, Blocken, de Coo, & Janssen, 2015; Wang, Wang, & Ng, 2021; Yang, Shi,

---

* Corresponding author.
E-mail address: joanna.badach@pg.edu.pl (J. Badach).
[1] Now at: Department of Chemistry, University of Oslo, P.O. Box 1033-Blindern, 0315 Oslo, Norway

---

Nomenclature

PM10 Yearly avg.   yearly average PM10 concentration [μg/m^3]
PM10 Min.   yearly minimum PM10 concentration [μg/m^3]
PM10 Max.   yearly maximum PM10 concentration [μg/m^3]
PM 10 L > 50 (S24)   number of days in the year in which the average 24-h PM10 concentration exceeded the standard level of 50 μg/m^3, rounded up to the nearest higher integer value [−]
λ_P plan area density [−]
λ_{PHM} plan area density – heterogeneity measure [−]
λ_{GFA} gross floor area ratio [−]
μ_H average height [m]
σ_H height variability [m]
μ_V mean building volume [m^3]
O_C occlusivity [−]
FAI   Frontal Area Index [−]
RTI   Residence Time Index [−]

Zheng, Shi, & Xia, 2020) but some account for a larger scope, e.g. the scale of an urban neighbourhood (Antoniou et al., 2017; Johansson & Yahia, 2020; Kurppa et al., 2018; Maing, 2022; Zhang et al., 2021). For the same reasons, urban geometry consideration in such studies is often limited to idealised and semi-idealised urban form models, producing relatively coarse meshes, such as generic building arrays (Acero et al., 2021; An, Wong, & Fung, 2019; da Silva et al., 2021; da Silva et al., 2022; Javanroodi, Mahdavinejad, & Nik, 2018; Peng, Gao, Buccolieri, Shen, & Ding, 2021; Qin et al., 2020; Ramponi et al., 2015; Wang et al., 2021). Studies involving more realistic urban models can be also found (Antoniou et al., 2017; Johansson & Yahia, 2020; Juan, Wen, Li, & Yang, 2021; Lauriks et al., 2021; Zhang et al., 2021) but are less common. To increase the simulation efficiency, the level of detail of the urban form model may be reduced to varying degrees, depending on the focus of the study (Mirzaei, 2021). Moreover, various model optimisation tools have been proposed (Chang, Jiang, & Zhao, 2018; Li et al., 2019). In the current research strong focus is also placed on increasing the simulations efficiency and developing more affordable numerical methods (Du et al., 2020; Rivas et al., 2019).

There persists a need to develop more CFD approaches which will facilitate the effective evaluation of the impact of urban form on air quality and advise the process of urban planning and design (Peng, Gao, Buccolieri, & Ding, 2019; Sefair, Espinosa, Behrentz, & Medaglia, 2019; Tian, Yao, & Chen, 2019). CFD simulations performed for a specific urban configuration, based on an existing case study, enable the identification of some local phenomena related to city breathability. For example, it is possible to identify zones characterised by low or high wind speeds at the pedestrian level (Ma & Chen, 2020; Zhang et al., 2021), pollution accumulation zones and air flow structures in urban neighbourhoods or blocks, or in street canyons (Lauriks et al., 2021; Yang, Shi, Shi, et al., 2020; Yuan et al., 2014). Apart from the model of an existing urban area, alternative design scenarios can be simulated and compared in order to select the most favourable in terms of the wind environment or air quality impacts (Jana, Sarkar, & Bardhan, 2020; Johansson & Yahia, 2020; Lauriks et al., 2021), including the analysis of on-going urban form transformation (Maing, 2022). Selected design elements can be also preliminarily tested on simplified models and, after establishing their impact on local air flow and pollution dispersion, they can be applied and investigated in more complex urban scenarios (An et al., 2019; Juan et al., 2021). The process of developing and selecting the most beneficial design can be also automated by means of dedicated optimisation tools (Ding & Lam, 2019; Kaseb et al., 2020). Such studies may lead to the development of some general guidelines and design solutions which enhance city breathability and local microclimatic

conditions (Badach, Voordeckers, Nyka, & Van Acker, 2020; He, Ding, & Prasad, 2019; Shi, Ren, Lau, & Ng, 2019; Voordeckers et al., 2021), including urban vegetation system management (Badach, Dymnicka, & Baranowski, 2020; Chun & Guldmann, 2018; Farhadi, Faizi, & Sanaieian, 2019; Van Ryswyk et al., 2019; Wojnowski et al., 2021). However, these guidelines are often context-specific and not easily applied in other urban areas (Badach, Dymnicka, & Baranowski, 2020; Poćwierz & Zielonko-Jung, 2021).

Another approach is to link the results of CFD simulations to urban form indicators. At the regional scale, landscape metrics and urban form parameters may serve as indicators of air pollution (F. Li, Zhou, & Lan, 2021; Łowicki, 2019; Tian et al., 2019; G. Xu, Zhou, Jiao, & Zhao, 2020). Similarly, at the local scale, certain urban form indicators can be identified as a proxy for the effectiveness of ventilation and pollution dispersion processes (Gao, Wang, Liu, & Peng, 2019; Liu, Chen, Wei, Wu, & Li, 2021; Voordeckers, Meysman, Billen, Tytgat, & Van Acker, 2021). In these studies the correlation between the on-site air quality data and the local urban land use and urban form features was analysed. This approach may be also used to link the features of the urban form and air quality data derived from of numerical simulations (Feng et al., 2020; Jia, Liu, & Ng, 2021; Yang, Shi, Zheng, et al., 2020). However, to the best of our knowledge, the majority of such studies, including the ones cited above, concern relatively high-density cities, in which the problems related to poor ventilation and increased pollution accumulation are most severe. Much fewer data are available for low-density cities or cities with more heterogeneous urban layouts. Therefore, these is a need to investigate cities with such characteristics. Another issue that needs to be addressed is the fact that it is not straightforward to link the results of CFD simulations to the urban form indicators. Usually, average values of the ventilation and pollution dispersion efficiency parameters within the investigated site are used (see e.g., Ma and Chen (2020), Peng et al. (2019)). Other parameters are developed such as the calm (or static) wind area ratio (the proportion of the area with wind speed below a certain value to the total site area) (Ma & Chen, 2020; Yang, Shi, Shi, et al., 2020), wind speed dispersion (the standard deviation of the wind speed at all selected points within the given area) (Ma & Chen, 2020), and the frequency of occurrence of favourable wind and air quality conditions between simulation runs (Mirzaei & Haghighat, 2012). More methods to conveniently derive a single continuous variable related to the effect of the urban structure on pollution dispersion from the CFD simulations are needed.

In this study, the issue of urban air quality in the shaping of the built environment was addressed with the aim of developing new tools and procedures facilitating urban air quality management. The adopted methodological approach (see Fig. 1) incorporated geographic information system (GIS) tools, 3D parametric modelling, and CFD simulations. In the last phase of the study statistical analysis was also applied. New CFD-based approach was proposed, inspired by the tracer method used in chemical engineering to calculate the Residence Time Distribution (RTD) (Rodrigues, 2021). It is a common CFD approach to study the flow patterns in various engineering and industrial applications (see, e.g. Chen, Bachmann, Bück, Jacob, and Tsotsas (2019), Adeosun and Lawal (2009), Aparicio-Mauricio, Rodríguez, Pijpers, Cruz-Díaz, and Rivero (2020)). However, to our knowledge, there are no previous applications of an approach inspired by the RTD for investigating air flow and pollution dispersion in urban areas. The adoption of this approach for such a purpose makes it possible to efficiently and robustly estimate the aerodynamic effects of the micro-scale urban form on pollution dispersion with a new singular index which can be conveniently juxtaposed with urban form indicators. By doing so, the results of the CFD study estimating the Particulate Matter (PM) dispersion and the historical PM concentrations can be conveniently compared to the GIS-derived micro-scale morphological indicators to examine which parameters of the urban form are most strongly correlated with the local wind environment and air quality in low-density urban areas.
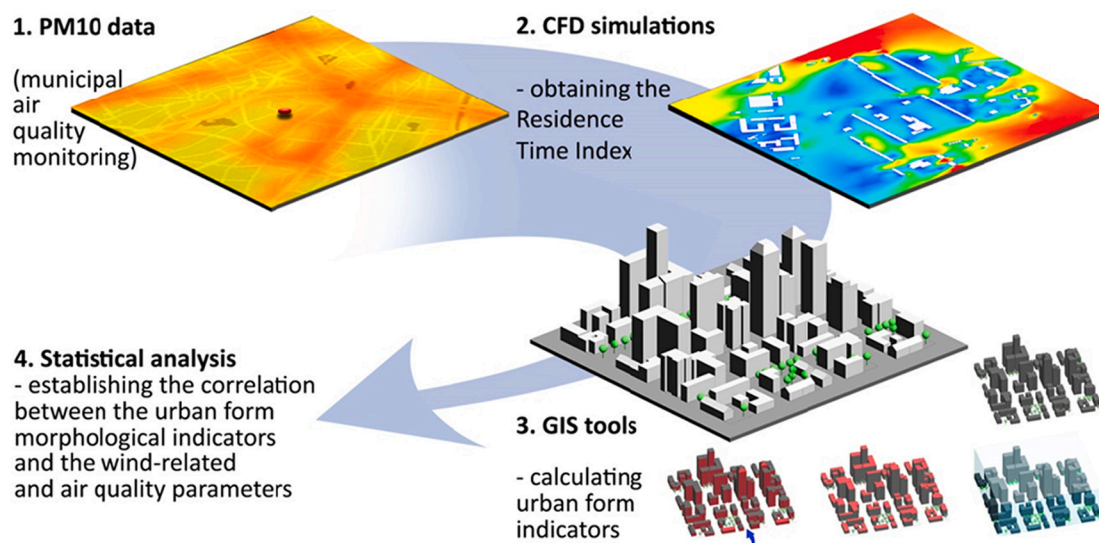
Existing heterogeneous urban segments around air quality

Fig. 1. Methodological approach used in the study.

monitoring (AQM) sites in three Polish cities – Gdańsk, Warsaw, and Poznań were investigated to validate the developed approach. Alarming reports published by the European Environment Agency (EEA) (2020) indicate that air quality management in Poland is highly inefficient. PM is one of the key pollutants related to urban and suburban air quality in Poland. This may be partly related to the energy policy based on coal combustion, the lack of investments in renewable energy sources, the out-dated infrastructure for household heating, and to traffic and industrial emissions (Gębicki & Szymańska, 2012; Łowicki, 2019). As of now, only scarce data regarding urban ventilation conditions and pollution dispersion with respect to the urban spatial structure, and especially more complex urban layouts, are available for Polish cities. Therefore, more studies are needed for cities with varied low-density urban form typologies but affected by significant air quality issues. This also pertains to the local urban conditions, legal requirements, and design practices in Poland, where urban air quality management is not sufficiently investigated and implemented in planning practice (Badach, Dymnicka, & Baranowski, 2020; Poćwierz & Zielonko-Jung, 2021). Moreover, the AQM network in Poland is not satisfactory, as currently there are only just over 100 monitoring sites within the state environmental monitoring system (Rogulski & Badyda, 2019). Another issue is related to the representativeness of these monitoring sites.

The representativeness of urban AQM systems is usually evaluated at the city or regional scale, by taking into account air pollution characteristics and factors such as human exposure to pollution, population density, or the concentration of emission sources (traffic or industry) (Alsahli & Al-Harbi, 2018; Henne et al., 2010; Piersanti, Vitali, Righini, Cremona, & Ciancarella, 2015). From the perspective of urban planning, spatial representativeness is particularly important as its aim is to establish the spatial extent, to which the obtained measurements are relevant, also in relation to the characteristics of the urban form (Janssen et al., 2012; Righini et al., 2014). The local morphological features of the urban form should also be taken into account while evaluating the representativeness of AQM sites as the measurements performed at certain stations may be considerably affected by local building configurations (Duyzer, van den Hout, Zandveld, & van Ratingen, 2015). CFD simulations are a suitable and accurate tool for such an assessment (Rivas et al., 2019; Santiago, Martín, & Martilli, 2013; Solazzo, Vardoulakis, & Cai, 2011). It usually involves comparing the pollution concentrations at the AQM locations to pollution concentrations modelled for their surroundings (Santiago et al., 2013). This approach also reveals whether any local pollution hotspots (or stagnant zones) are not accounted for in the process of AQM. However, it involves conducting a set of simulations for different seasons and meteorological conditions, which is computationally expensive and time-consuming. Therefore, there is a need to account for the impact of the spatial characteristics of the monitoring site on the local dispersion of pollutants in a more convenient way. The issue of using the proposed approach for the evaluation of the local spatial representativeness of AQM sites, accounting for the morphological features of the urban form, was also addressed in this study.

2. Methods

2.1. Study areas – PM monitoring sites

The municipalities selected for the study – Gdańsk, Warsaw, and Poznań, – exhibit heterogenic topography, urban morphology, land use, and vegetation systems. As such, they were chosen as representative of various spatial structures in order to test the developed method in different scenarios. Gdańsk (54.35° N, 18.65° E) is a city on the Baltic coast, Warsaw (52.23° N, 21.01° E) - on the Vistula river, and Poznań (52.41° N, 16.92° E) - on the Warta river. For more details about the cities see: Badach, Dymnicka, and Baranowski (2020). A total of 15 AQM sites conducting PM10 measurements in Gdańsk, Warsaw, and Poznań were included in the study. Their locations are depicted in figs. A.1, A.2, and A.3 in Appendix A. Descriptions of the stations and their surroundings are included in tables B.1, B.2, and B.3 in Appendix B.

Year 2019 was considered in the study as in previous years some of the AQM sites were not yet in operation. The following PM10 data were retrieved from the measurements databank of the Main Inspectorate of Environmental Protection GIOŚ in Poland (2021): yearly average PM10 concentration (PM10 Yearly avg.), yearly minimum and maximum PM10 concentrations (PM10 Min and PM10 Max), and the number of days in the year in which the average 24-h concentration exceeded the standard level of 50 $\mu g/m^3$, rounded up to the nearest higher integer value (PM 10 L > 50 (S24)) (see Appendix C). Moreover, the averaging time for each station was given, as well as the total number of measurements and the measurements' completeness. In the case of the G4 station, there is a reference container station and a free-standing PM sampler at the same location. The data from the reference station were considered. Moreover, in case of some of the stations, the PM10 statistics were given with the averaging times of both 1 h and 24 h. In such cases, the statistics with the averaging time of 1 h were considered. If they were not available, the statistics with the averaging time of 24 h were considered.

2.2. CFD simulations

2.2.1. Parametric modelling of urban form

3D models of the built environment (see Fig. 2) were developed for the purpose of the CFD simulations by means of GIS and computer aided design (CAD) tools. A buffer of 400 m was used for each AQM point to delimit the area for the analysis. This follows the well-established practices and falls within the similar range applied in studies evaluating the impact of urban form on air quality at the urban micro-scale (Antoniou et al., 2017; Ding & Lam, 2019; Maing, 2022). More importantly, the dimensions of the computational domain were based on the relevant best practice guidelines (see the following subsections). Only the buildings' layouts were modelled; other elements of the built environment were not considered. 2D data were used, especially since very detailed building geometries are not required for CFD simulations and would inflate the mesh density without increasing the model's accuracy. This follows an established practice in which design details are neglected and considerable model simplifications are applied, improving the efficiency of the simulations. Therefore, the buildings were modelled as simple extrusions according to their approx. height, without applying building geometries and other elements (as in, e.g. An et al. (2019); Jana et al. (2020); Johansson and Yahia (2020); Maing (2022); Yang, Shi, Shi, et al. (2020); Zhang et al. (2021)).

The geospatial datasets were acquired from the Head Office of Geodesy and Cartography (2019). Using 3D City GML building models was also considered but these models were not up-to-date and a different Level of Detail (LoD) was available for the three cities. The datasets were first processed with ArcGIS Pro v2.8 (Esri, USA). The 'Simplify Building' geoprocessing tool was applied when necessary in order to limit the number of elements in the CFD simulations (see the following section). It simplifies the polygons that make up the buildings' footprints while maintaining their general size and shape (Esri, 2021). If only a minor part of a building was left at the boundary of the applied buffer, such building was omitted. The buildings were then extruded from the 2D outlines based on their elevation using CAD software. Since more detailed information about the buildings' heights is not available in the database, an average height of the building story was assigned, following Wang, Cot, Adolphe, Geoffroy, and Sun (2017) or Badach, Voordeckers, et al. (2020), and it was fixed at 3.5 m. For buildings with a more complex structure, such as e.g. historical buildings, for which the number of floors does not apply, the height was estimated based on site images. Finally, the buildings models were subtracted from a larger fluid (air) domain (2000 × 800 × 250 m, oriented with the shorter edge along the wind direction – for the West (W), East (E), North (N) and South (S) directions).

2.2.2. Validation

The simulations were carried out using Autodesk CFD 2021. This software is increasingly commonly used for the evaluation of airflow and air quality in urban areas due to its convenient integration with 3D modelling and other environmental simulation tools, and its good performance, e.g. on par with the well-established ANSYS Fluent (Javanroodi & Nik, 2020; Johansson & Yahia, 2020). The simulation parameters such as mesh density, turbulence model, meshing parameters, and the number of wall layers were validated according to the Architectural Institute of Japan's (2016) guidelines for CFD predictions of urban wind environment. In particular, the Niigata dataset containing the results of field measurements within a building complex in an actual urban area, with simplified building outlines, was chosen as the benchmark due to its similarity to the scale, complexity, and topology of the investigated scenarios (Architectural Institute of Japan, 2008). The models performance was evaluated by comparing the real city case and the corresponding data with the results obtained using the computational model with the settings which were used in the subsequent scenarios. The size and shape of the domain as well as the boundary conditions (wind velocity profile) were based on the above-referenced dataset and case study. The optimised model validation results were on par with the results previously reported for the same dataset (Lynch,
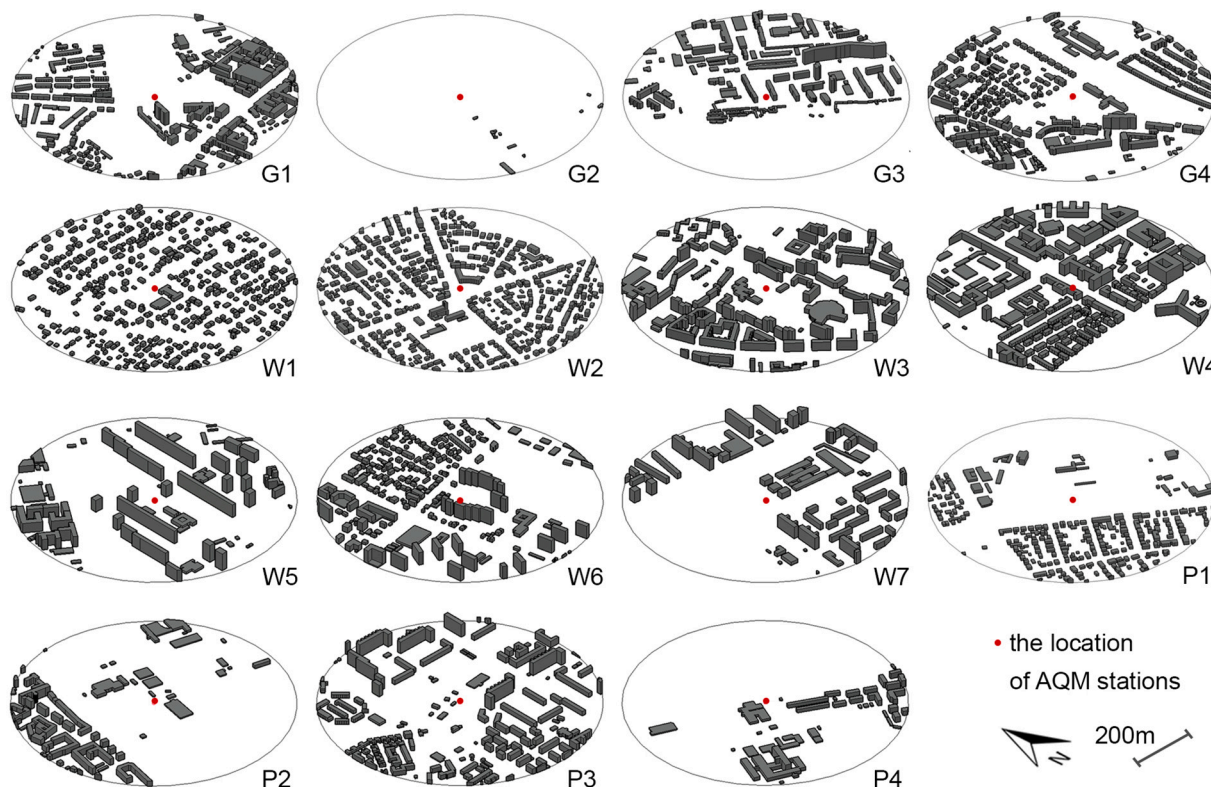

Fig. 2. Simplified models of the urban segments surrounding AQM sites.

2018) (see Fig. D1, Appendix D).

2.2.3. Setup and boundary conditions

The 3D models of the built environment were imported into Autodesk CFD via Autodesk Fusion 360. The mesh was parametric and generated automatically with no iterative refinement, with a minimum of four points along an edge. To more accurately model the flow along the ground and between the buildings, the number of wall layers was set to six (six layers inflated relative to the cell size). The simplification of the buildings layout applied in the previous step kept the number of elements for each model below 1 mln. The number of elements varied in each scenario with the density of the built environment, and is listed in Appendix C. Steady-state model was used together with the standard air material. The k-ε turbulence model was chosen based on the validation results. Due to its robustness, it is the turbulence model which is most commonly used for assessing the fluid dynamics in a built environment (Chen et al., 2017; Lin, Hang, Li, Luo, & Sandberg, 2014; Peng et al., 2019). The inlet boundary condition was defined as velocity with linear variation, defined by a log wind velocity curve with 2.85 m•s^{-1} at 1.25 m and 7.80 m•s^{-1} at 250 m. The outlet was assigned a zero gage pressure condition, and the three sides were slip walls (Fig. 3). The ground and building walls were assigned a no-slip condition. The simulation settings were in line with the COST Action 732 recommendations, with blockage of <3% in all scenarios (Britter & Schatzmann, 2007). Four RANS simulations per model (one per cardinal direction: N, S, E, W) were run to a tight convergence, which in most cases took between 500 and 800 iterations.

2.2.4. Assessment of the impact of the urban form on PM10 retention

There are several approaches to extracting a single variable based on the results of a CFD flow simulation within a domain representing built environment, as it was previously discussed. Perhaps the most straightforward approach in this study would be to account for the atmospheric pollution when defining the boundary condition by assigning a scalar mixing condition to the inlet and defining the initial concentration of PM10. The value of the scalar could then be extracted from the simulation results at several points in the vicinity of the AQM station and averaged. However, this would involve treating particulate matter as a gaseous substance instead of an aerosol, and would also introduce

difficulties with selecting representative reference points within the model. Therefore, the RTI was proposed. Following the successful approximation of the solution of the N-S equations during the CFD simulations, a set of tracers was introduced within the simulation domain, upwind from the model of the built environment. Each of the 200 tracers was intended to represent a PM10 particle, and they were assigned the density of 1.65 g•cm^{-3} (Liu et al., 2008), diameter of 10^{-5} m (the size of the largest PM10 particles), and the coefficient of restitution of 0.47 (Yardeny, Portnikov, & Kalman, 2020). The effect of gravity was intentionally not accounted for. This on the one hand lowers the fidelity of the estimation of the behaviour of the particles, but on the other hand isolates the effect of the built environment and makes the result independent of the scale of the simulation domain.

The tracers were introduced (seeded) at the height of 2 m, mid-way between the inlet and the model of the buildings, i.e. 300 m from both the edge of the domain and the models of the buildings (see Fig. 3). The 200 tracers spanned 400 m centred at the axis of the domain, with 2 m spacing between each seed. The result of this operation was the ratio of the tracers that penetrated the model of the built environment, as shown in Fig. 4. For instance, the ratio would equal 1.0 if none of the tracers were retained within the model of the built environment, 0.5 if half were retained and half penetrated the model, and 0.0 if all of the tracers were retained within the model due to its density or the aerodynamic properties of the flow within the model. The calculated values of the Residence Time Index (RTI) for each AQM site are available in Appendix C. The motivation behind using the RTI was the need to derive a single continuous variable from the CFD simulation that would be related to the effect of the urban structure on the dispersion of pollutants. It had to be valid for the whole area in question so that it could then be juxtaposed with the GIS-based indices. It should be noted that it does not simulate the actual dispersion of externally introduced particulates within the domain, but is instead intended to isolate the contribution of the effect of the built environment on the dispersion of particulate pollution.

2.3. GIS analysis

A GIS analysis was performed in ArcGIS Pro to calculate the urban form indicators for each AQM site. The approach to identify the urban
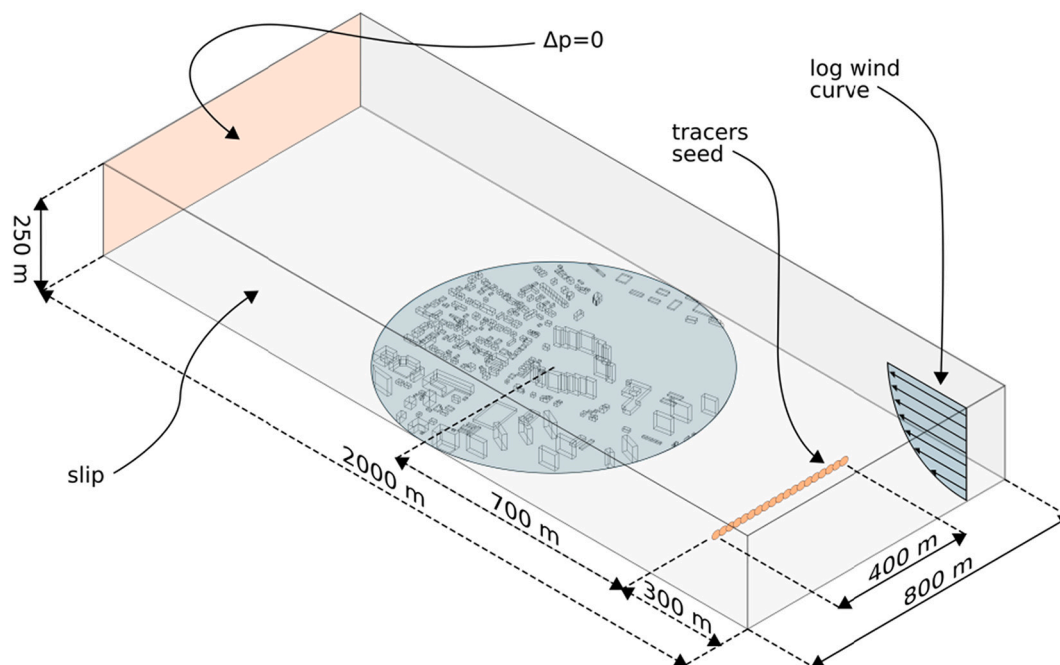

Fig. 3. Simulation domain and boundary conditions for the CFD simulations.
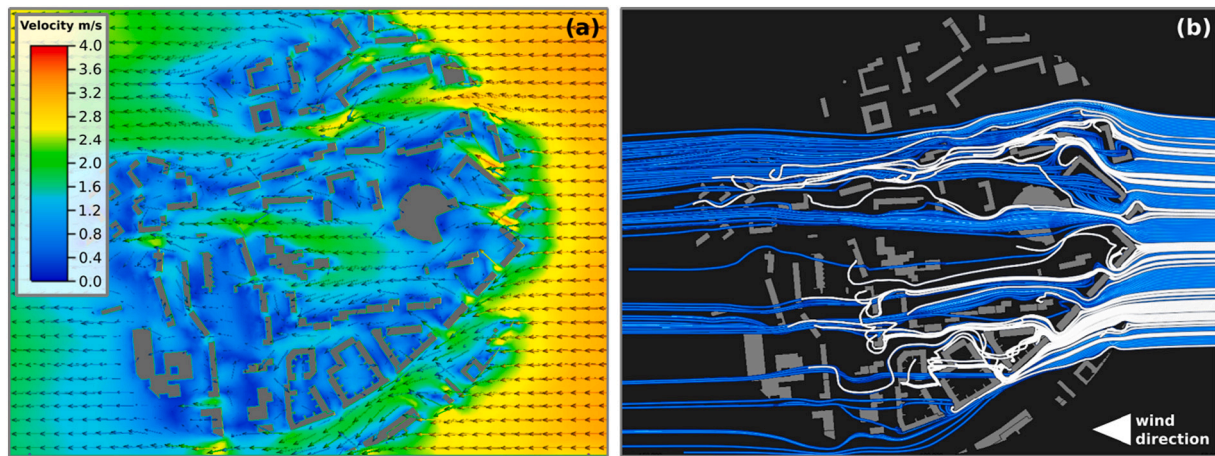
Fig. 4. (a) Simulated velocity magnitude at 2 m in the W3 model with easterly wind; **(b)** corresponding PM10 tracers, with 150 tracers penetrating the model (blue tracers) and 50 tracers retained by it (white tracers) producing an RTI of 0.75. (For interpretation of the references to colour in this figure legend, the reader is referred to the web version of this article.)

form typologies that have an impact on ventilation and pollution dispersion was described by e.g. He et al. (2019) and Badach, Voordeckers, et al. (2020). In these studies, the urban morphometric indicators were quantified for the city or neighbourhood scale, e.g. using grid-based analysis. However, in this case, the urban form indicators were calculated for selected urban segments, which can be treated as corresponding with a single grid cell. The same dataset and the same height approximation were used as for the development of the 3D models but buildings' footprints were not simplified. The spatial scope for the analysis was consistent with the CFD study – a buffer of 400 m was applied for each point. The calculations were automated by dedicated Model Builder toolboxes, developed for the purpose of the study.

Selected indicators relevant to this study were based on Badach, Voordeckers, et al. (2020), namely: plan area density (λ_P), gross floor area ratio (λ_{GFA}), and height variability (σ_H). λ_P was calculated as the ratio between the total buildings footprint area and the site area. λ_{GFA} was calculated as the ratio between the sum of all building floor areas and the site area. σ_H was calculated as the standard deviation of the buildings' height on the site. The average height (building footprint area weighted) (μ_H) was also calculated. Standard geoprocessing tools were used to calculate each indicator, in particular the 'Summarize Within' tool which summarises the selected elements or their features within the given polygon (Esri, 2021).

Further indicators relevant to the urban micro-scale found in literature were also used. As suggested by Liao, Hong, and Heo (2021), the impact of the spatial heterogeneity of the urban forms on the environmental performance should be considered alongside the average values of the urban spatial variables. Therefore the heterogeneity measure, defined as the standard deviation measure of the spatial variables, was also included. Specifically, the plan area density heterogeneity measure (λ_{PHM}) was calculated by dividing each polygon into 25 smaller, equal-sized parts (strips). For each polygon part, the values of the λ_P were then calculated using the same approach as for the undivided polygon. In the final step, the 'Summarize Within' tool was used to calculate the standard deviation of the λ_P for all of the polygon parts. The values of the indicator close to 0 stand for a uniform layout of built-up structures. The higher the values of λ_{PHM}, the more uneven the layout. It is important to note that although the calculation was performed for parts (strips) aligned in the N/S and E/W directions similarly to the setup of the CFD study, the λ_{PHM} is not a wind-related parameter.

Next, an indicator used to describe the dispersion level of buildings with different heights – mean building volume (μ_V), described by Wang et al. (2017) – was calculated as the ratio between the sum of buildings volumes on the site and their number using the 'Summarize Within' tool.

Finally, an indicator to account for the openness of the urban segments to the sky was included. This feature is most commonly described by means of the sky view factor (SVF), which measures how much sky is visible at a given location by establishing the ratio between the areas open to the sky and the total area of a hemisphere around a given point (Dirksen, Ronda, Theeuwes, & Pagani, 2019; Middel, Lukasczyk, Maciejewski, Demuzere, & Roth, 2018; Xu et al., 2017). However, SVF is more suitable for local-scale analysis, at scales below 100 m (Dirksen et al., 2019). Therefore, the occlusivity (O_c) indicator was used (Wang et al., 2017). It was calculated as the mean ratio between the built-up area (the sum of the buildings' footprint areas) and the open area for a given horizontal section. Due the standard building floor height, one section was applied every 3.5 m with the total of 16 sections (the maximum number of floors in the investigated urban segments). The relevant ratios between the built-up area and the open area for each section and then their the mean value was calculated using 'Summarize Within' tool after grouping the buildings according to their number of floors. O_c values close to 0 are obtained for almost open areas and the higher the O_c values, the more limited the openness to the sky.

In addition to the CFD-based RTI, another parameter that account for the relationship between urban geometry and the wind environment was considered. Frontal area index (FAI) (or frontal are density), calculated as the ratio between the projected area of the buildings façades facing the selected wind direction and the site area, describe the three-dimensional permeability of the urban form. At the city scale, it is successfully applied to urban ventilation efficiency assessment as it makes it possible to identify ventilation corridors – passages through the urbanised areas facilitating undisturbed airflow and pollution dispersion, also contributing to the improvement of the urban thermal environment (Ren et al., 2018; Wong, Nichol, To, & Wang, 2010). It is also used at the urban micro-scale as one of the urban morphology parameters potentially affecting pollution dispersion capabilities (da Silva et al., 2021; Li, Zhang, Wen, Yang, & Juan, 2020). It is important to note that although both RTI and FAI, in contrast to the rest of the GIS-based urban form indicators, are wind-related, they describe urban morphology and its relationship with the ventilation conditions and the process of pollution dispersion (in a sense, the permeability of the urban form). While the proposed RTI more accurately accounts for the aerodynamic effect of the urban micro-scale form on the pollution dispersion, FAI is easier and more straightforward to calculate using only GIS tools. In high-density urban environment, FAI was linked with pollution dispersion (Shi, Xie, Fung, & Ng, 2018). It should be determined if it is also the case in low-density urban areas. The values of FAI were derived for the urban segments by creating flatshots of the models used for the

CFD simulations (in the W-E and N-S directions) and calculating the ratio between the total buildings frontal area and the site area.

2.4. Statistical analysis

In the final phase of the study, statistical analysis was conducted to identify which features of urban form are correlated with the results of the CFD simulations describing pollution retention within urban segments. This was done to assess which features of the urban form in the low-density urban environment have the strongest impact on pollution retention. Since RTI describes the combined impact of the entire urban segment, it is necessary to isolate particular indicators which have the strongest role in shaping the dispersion of pollutants.

The main goal at this stage was to assess the correlation between urban form indicators and RTI, as the latter comprehensively accounts for the interaction between the geometrical characteristics of the urban form and the wind environment, albeit at a higher computational cost. However, it was also interesting whether the FAI values are similarly linked with the urban form indicators not related to the wind direction. Therefore, the correlation between FAI and the remaining urban form indicators was also evaluated.

Finally, the correlation between urban form indicators and PM10 data was investigated. However, given the fact that yearly PM10 values were used, while the CFD simulations were carried out in the steady state and do not reflect temporal shifts in conditions, significant link was not expected to be discovered in this case. Furthermore, the PM10 data are obtained from a single fixed point (AQM station) in the centre of the domain, and the RTI does not represent the actual dispersion of PM10, but the isolated effect of the built environment on 10 μm particles. In a less complex and more repeatable case scenario, such as an urban street canyon, it is easier to find a correlation between the parameters on the urban morphology and the air quality data (Voordeckers, Meysman, et al., 2021) than in much more complex scenarios such as the investigated selection of urban segments. Statistical analysis was used to confirm this.

A Pearson correlation analysis was conducted to establish which urban form indicators have the strongest correlation with the wind-related RTI and FAI, and the PM10 data. It is important to note that in case of the RTI, the datasets included four different objects for each of the 15 stations, in the case of FAI – two objects, and for the PM10 measurements – one object.

3. Results

The GIS analysis confirmed that a varied selection of urban forms, derived from the existing Polish cities, was investigated in the study (see Appendix C). However, with the value of λ_P up to 0.243 (for station W4) and the value of λ_{GFA} exceeding 1.0 only slightly in one case (1.024 for station W4), all of the urban segments can be classified as low-density, with relatively sparse or medium λ_P (for comparison see e.g., An et al. (2019), Badach, Voordeckers, et al. (2020), da Silva et al. (2021), Wang et al. (2017), Yu, Liu, Wu, Hu, and Zhang (2010)).

On the other hand, they are rather varied in terms of the layout of the built-up structures and their height variability. The σ_H varied between 0 (station G2) and approx. 17 m (station W5). The λ_{PHM} was also varied (with the lowest value of 0.005 (N/S direction) at station G2 – although this segment is not a good example as it is an almost non-built-up area, then 0.021 (W/E direction) at station W2 (with a relatively even layout of small buildings) to 0.112 (W/E direction) at station W4 (with densely built-up structures in the northern and central part of the segment and open area in its southern part). These values of the λ_{PHM} are, however, hard to place in the context of previous studies as this indicator has rarely been applied in the literature. In a study by Liao et al. (2021), the λ_P heterogeneity measure for the entire areas of the investigated cities was 0.09 and 0.12, and for the scope of an urban neighbourhood, values of up to 0.24 were calculated. Moreover, this measure is heavily

dependent on the way the main polygons are divided into smaller parts.

The visualization of the simulation results showing the wind velocity magnitude for all investigated urban segments at 2 m above the ground are depicted in Fig. 5 (the location of the AQM stations for each visualization is indicated by a red dot). Various urban micro-scale ventilation phenomena can be observed such as ventilation paths, characterised by higher wind velocities, and stagnant zones around the buildings or in the buildings' courtyards. For example, relatively long buildings can cause unfavourable ventilation conditions. When the wind direction is perpendicular to the longer façades, stagnant zones are created alongside their longer edges, while zones characterised by high wind velocities, causing pedestrian wind nuisance, are created at their shorter edges. It can also be concluded that in urban segments with relatively even layout and small-scaled buildings, relatively stable ventilation conditions occur.

The identification of such phenomena can be used to propose design measures to mitigate unfavourable conditions. For example, in order to reduce the accumulation of pollution in the stagnant zones, building voids, spacing between buildings, or ground floor openings may be proposed (Du & Mak, 2018). Then the modified urban layout should be re-evaluated using the CFD approach and further mitigation measures may be proposed until satisfactory conditions are obtained (Jana et al., 2020; Johansson & Yahia, 2020; Lauriks et al., 2021). However, such an analysis, being related to the specific case study, was not the main purpose of the investigation. The RTI was the most important parameter derived from the CFD study, and its values were further used to investigate the impact of the micro-scale urban form on pollution dispersion. Once the urban morphological indicators significantly correlated with the wind-related and air quality parameters are identified, they can be applied in the process of air quality management.

To evaluate the impact of the urban micro-scale form on pollution dispersion, a pairwise Pearson correlation analysis was used. Tables 1 and 2 show the correlation coefficients (r) between the urban form indicators and the wind-related parameters as well as between the urban form indicators and the PM10 measurements (their values are listed in Appendix C). The positive r-values mean positive correlations and the negative r-values mean negative correlations. The absolute value of r varies from 0 to 1, where 0 means no correlation and 1 means full correlation. Bold typeface denotes r-values higher than 0.4 (moderate correlation between 0.4 and 0.59, strong correlation between 0.6 and 0.79, and very strong correlation between 0.8 and 1) for a false discovery rate (FDR) lower than 0.05. It should be noted that statistically significant correlations between urban form indicators and air quality or wind-environment parameters even above 0.3 should be considered relevant in complex scenarios such as urban environments, with a plentitude of independent variables, where numerous other variables are necessarily not accounted for (see e.g., Voordeckers, Meysman, et al. (2021). While the dataset contained dependent, strongly correlated variables, such as e.g. λ_{GFA} and O_c ($r = 0.997$, FDR $= 3.39e^{-14}$), that was not the case when examining the correlation of urban form indicators with wind-related or air quality parameters.

Based on the statistical analysis, we can see that:

1. RTI is strongly correlated with λ_P ($r = -0.686$), and moderately correlated with λ_{GFA} ($r = -0.418$) and O_c ($r = -0.431$). Such a strong negative correlation between RTI and λ_P can be easily explained by the fact that when the value of λ_P increases, the pollution retention within the urban segments increases due to the reduced amount of open space for pollution dispersion, so consequently the value of RTI decreases. It can also be easily explained that, since RTI is calculated based on tracers introduced at the height of 2 m (the height of the pedestrians but also AQM), it is well-correlated with building plan-related indicators. However, it is not significantly correlated with the building height- and volume-related indicators (μ_H, σ_H, μ_V). The lack of a correlation with λ_{PHM} is not that straightforward to explain and requires further investigation.
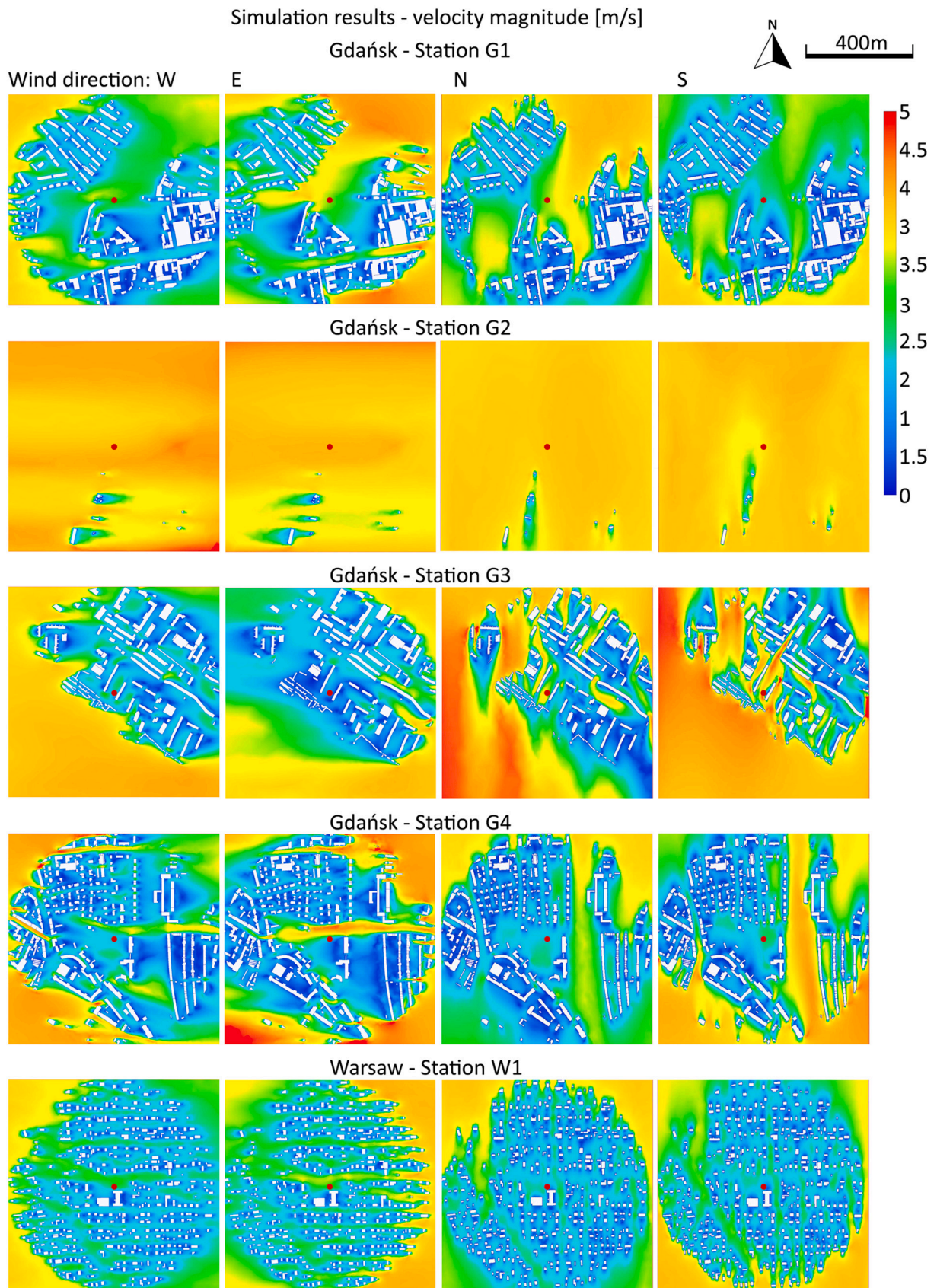
Fig. 5. CFD results – wind velocity magnitude of the urban segments models in four wind inlet directions.
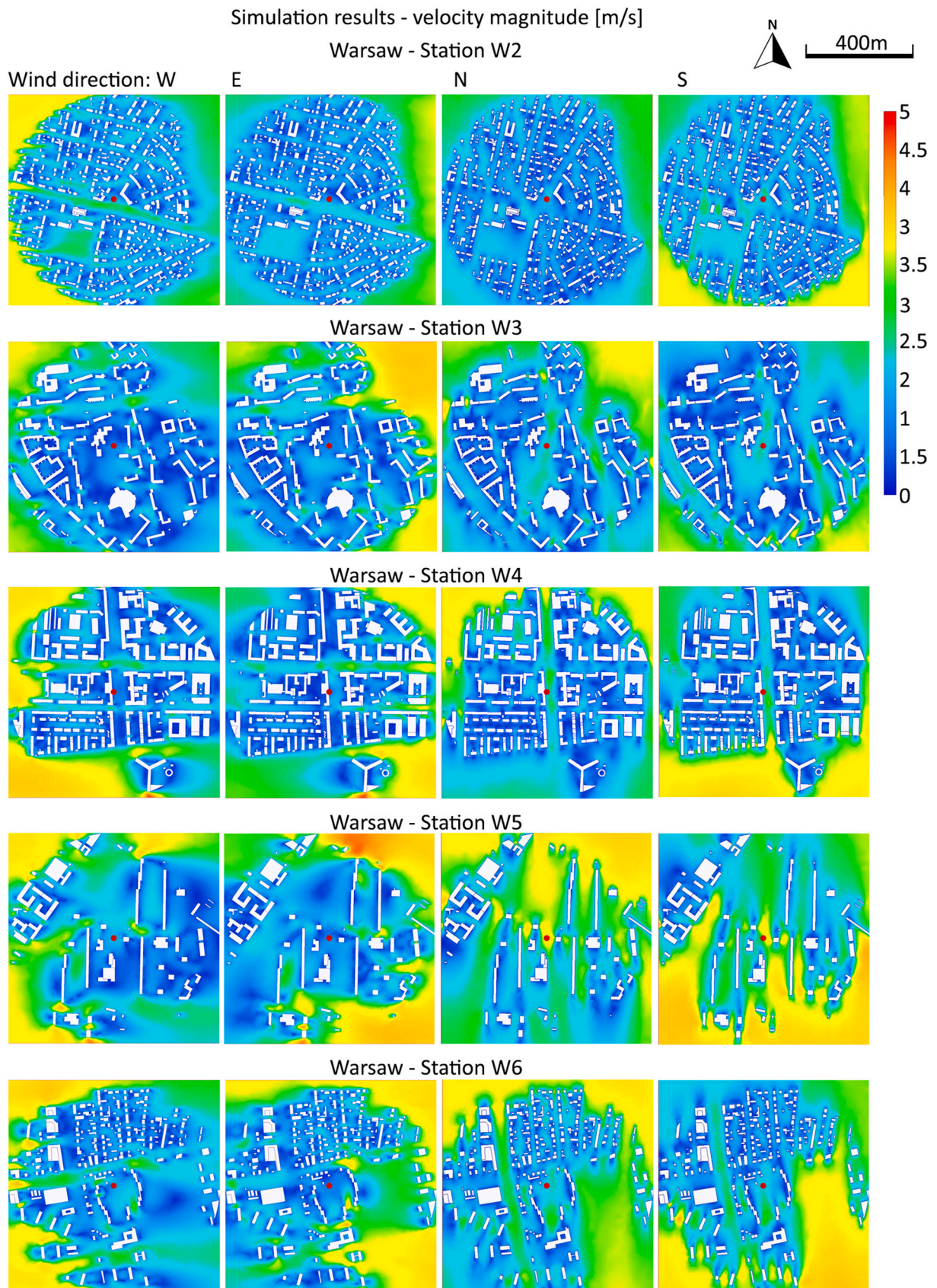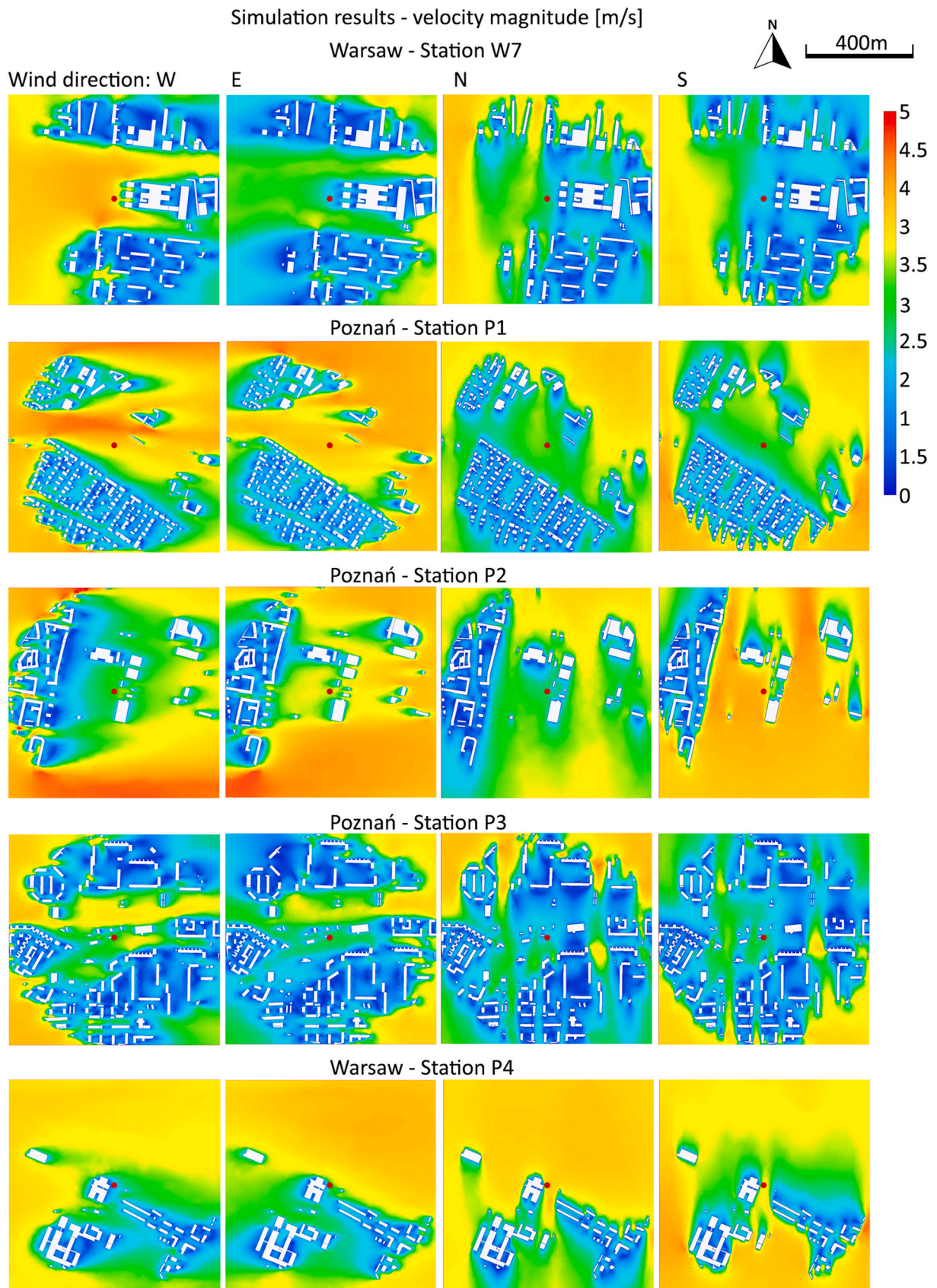
Fig. 5. (*continued*).

Fig. 5. (*continued*).

Table 1

Pairwise Pearson correlation coefficient (r) between the indicators of the urban form and the wind-related parameters.

Urban form indicators	Wind-related parameters			
	RTI		FAI	
	r	FDR	r	FDR
λ_P	**−0.686**	$9.95E^{-09}$	**0.572**	0.001
λ_{PHM}	−0.161	0.382	**0.412**	0.024
λ_{GFA}	**−0.418**	0.002	**0.856**	$5.67E^{-09}$
μ_H	−0.125	0.403	**0.904**	$5.28E^{-11}$
σ_H	0.015	0.91	**0.811**	$9.84E^{-08}$
μ_V	0.124	0.403	**0.651**	$1.37E^{-04}$
O_c	**−0.431**	0.002	**0.82**	$6.9E^{-08}$

2. FAI is significantly correlated with all building form indicators, and in every case the correlation is moderate, strong or very strong. This is not in line with what was found for RTI. Since RTI more accurately captures for capturing the effect of the buildings configuration on pollution dispersion, the discrepancy of the results indicates that FAI only vaguely accounts for the local wind environment in case of heterogeneous and complex urban scenarios. Although it is very useful in some cases, especially in the city-scale analysis, and it can be easily calculated using GIS or CAD tools, it seems that its application at the urban micro-scale for the purpose of evaluating the breathability and the representativeness of AQM sites should not be considered.

3. No strong significant links between PM10 measurements and the urban form indicators were found (with the exception of λ_{PHM} which was strongly correlated with **PM 10 L > 50 (S24)** ($r = 0.63$)).

4. Discussion and urban policy implications

Many CFD studies performed on models of existing urban areas are aimed at characterising the local phenomena related to the process of urban ventilation and pollution dispersion. The outcome of such studies can inform the urban planning and design process by identifying how particular urban form scenarios effect air flow and pollution accumulation in the urban built environment. However, such evaluation brings results relevant only to the specific case study. This study was not focussed on characterising the impact of design measures on ventilation and pollution dispersion processes within the selected urban segments. The conducted CFD simulations could serve this purpose but simply doing so does not provide versatile planning and design implications. On the other hand, establishing the correlation between the morphological features of the micro-scale urban form and the wind environment or air quality parameters, either obtained be means of numerical simulations (Feng et al., 2020; Jia et al., 2021; Wang et al., 2020) or based on-site (measured) data (He, Ding, & Prasad, 2020; Shi et al., 2018; Voordeckers, Meysman, et al., 2021), is a valuable approach, bringing some general planning policy implications. Based on the results of such studies, the potential problem areas related to air quality and wind environment management in the given urban site can be later easily

identified using non-CFD methods (Badach, Voordeckers, et al., 2020; He et al., 2019; Ren et al., 2018; Yuan et al., 2019).

Therefore, the overall objective of the study was to identify the features of the urban form which are most strongly linked with the process of urban ventilation and pollution dispersion within low-density urban micro-scale layouts with relatively low λ_P. Such data may be already available for high-density urban areas (Li et al., 2020; Shi et al., 2018) but areas with different characteristics require further investigation. The results of this research could facilitate the formulation of more conscious policies and spatial strategies in terms of monitoring and improving urban air quality in Polish cities and cities characterised by similar spatial conditions. For example, this study shows that in the investigated context, the indicators most strongly linked to pollution retention are λ_P, λ_{GFA}, and O_c. While the first two are already widely used in the local planning practice in Poland (especially to determine the parameters of the permitted intensity of new developments in the local spatial development plans – the basic planning regulations at the level of urban blocks and neighbourhoods), the use of the **Oc** which describes the openness of the urban form, is not common. This indicates the need for including a more varied selection of urban form indicators in local planning and adjusting their thresholds with respect to city breathability. Although it requires further research to definitely determine the most beneficial thresholds in various scenarios, this study can serve as a methodological basis for such analysis.

It is important to note that apart from including additional parameters to supplement planning provisions, the CFD analysis should be required in critical case scenarios. Such practice is already recommended in some urban areas, especially at the early stage of urban design (see, e.g.the guidelines developed by the City of London (2019). Therefore, most importantly, this study has more general validity. The proposed CFD approach may particularly relevant for shaping urban policy with respect to improving city breathability and air quality. It especially applies to the development of a single parameter that can successfully characterise the pollution retention capabilities of the urban micro-scale form, the CFD-based RTI, without the need to run a set of time-consuming and computationally-expensive simulations for different seasons and meteorological conditions. This is very convenient for comparing various urban areas and discussing the transferability of planning policies in the process of policy-making.

Another important policy implication may be drawn from this study. It was demonstrated that the available PM10 data are rather poorly linked with the urban form indicators. This confirms that in such complex urban scenarios the pollution concentration values measured at a single point are not sufficient for shaping the spatial policy. A higher spatial resolution of air quality data is particularly important from the point of view of urban air quality management and its integration with spatial development of urban areas. Therefore, there is a need to extend the current AQM network in Poland, and to this end, the potential of low-cost sensing technologies should be considered (Barcelo-Ordinas, Garcia-Vidal, Doudou, Rodrigo-Munoz, & Cerezo-Llavero, 2018; Gębicki & Szymańska, 2012; Wang et al., 2016).

Finally, the use of the proposed approach for evaluating the local

Table 2

Pairwise Pearson correlation coefficient (r) between the indicators of the urban form and the PM10 measurements.

Urban form indicators	PM10 measurements (2019)							
	PM10 yearly avrg.		PM10 Min.		PM10 Max.		PM 10 L > 50 (S24)	
	r	FDR	r	FDR	r	FDR	r	FDR
λ_P	0.513	0.177	0.311	0.315	0.099	0.791	0.38	0.229
λ_{PHM}	0.62	0.096	0.46	0.148	0.075	0.791	**0.63**	0.037
λ_{GFA}	0.303	0.476	0.382	0.218	−0.264	0.598	0.182	0.595
μ_H	−0.024	0.932	0.273	0.379	−0.557	0.108	−0.113	0.703
σ_H	−0.157	0.807	0.126	0.706	−0.572	0.108	−0.237	0.502
μ_V	−0.108	0.819	0.048	0.864	−0.448	0.219	−0.153	0.631
O_c	0.345	0.476	0.389	0.218	−0.216	0.616	0.226	0.508

representativeness of AQM sites in relation to urban spatial structure should be considered. The process of air pollution dispersion in urban areas is affected by the local wind environment, which is in turn governed to a significant extent by the urban morphology. Therefore, the concentration of pollutants captured by urban stations is affected by the permeability of the surrounding urban form geometry. The proposed new methodological approach can also be useful to investigate how local urban form characteristics affect the results of AQM, enhancing the evaluation of the spatial representativeness of AQM sites. RTI as a measure of the pollution retention capability of urban layouts can be used to effectively determine, without the need to perform long-term simulations with the use of extensive input data, whether a particular site is prone to pollution accumulation or, on the contrary, if it is porous, allowing for more effective pollution transport. The value of RTI for a particular site gives more general, but more easily comparable result. By deriving and comparing this index for the closest surroundings of an AQM site and the adjacent areas, we can instantly obtain information whether some local disturbances in the transport of pollutants occur such as the above-mentioned accumulation of pollutants. Moreover, since it is calculated for a particular spatial range, it can be conveniently juxtaposed with other parameters currently used in the evaluation of the local spatial representativeness of AQM sites, such as the population distribution, the exposure of inhabitants (Santiago et al., 2022), or other population-health based metrics (Hohenberger, Che, Fung, & Lau, 2021). However, this issue was not explored in depth in this study so more research is needed to determine how the RTI is advantageous for the representativeness of AQM sites. It remains to be determined in further research which RTI threshold values are relevant for evaluating spatial representativeness, also by cross-comparing various AQM sites in many other case studies.

5. Conclusions

The objective of this study was to evaluate the impact of urban micro-scale form on the process of pollution dispersion. It was based on CFD simulations, and GIS and statistical analyses. A new CFD-based approach was proposed to characterise the aerodynamic effects of the buildings' form and layout on pollution retention within the urban built environment. The simulations were conducted using simplified 3D models of existing AQM sites in three Polish cities: Gdańsk, Warsaw, and Pozna as inputs, and they made it possible to establish and compare the local ventilation conditions in various urban block typologies. The impact of urban form on pollution dispersion and city breathability in low-density cities with relatively heterogeneous urban segments was robustly determined by means of the numerical simulations. However, the main focus of this study was to develop a new approach that makes it possible to evaluate the PM10 retention capability of the urban form.

The RTI was calculated for each site, describing the ratio between the set of tracers representing the 10 μm particles that penetrated the model of the built environment to the ones that were retained within the model. The potential of this approach for the determination of the representativeness of local AQM sites should be explored in further studies. GIS and statistical analyses indicated that various features of the urban form in the investigated conditions are moderately and strongly correlated with the wind-related parameters. FAI is significantly correlated with all building form indicators, but due to the discrepancy between these findings and the findings for RTI, which is a more accurate measure to capture the impact of urban form on pollution dispersion, FAI should not be considered an appropriate parameter to evaluate the breathability of the urban environment at the local scale and to be used for assessing the representativeness of AQM sites.

CRediT authorship contribution statement

Joanna Badach: Conceptualization, Data curation, Funding acquisition, Investigation, Methodology, Resources, Validation, Visualization, Writing – original draft, Writing – review & editing. **Wojciech Wojnowski:** Conceptualization, Data curation, Investigation, Methodology, Validation, Visualization, Writing – review & editing. **Jacek Gębicki:** Conceptualization, Funding acquisition, Supervision, Writing – review & editing.

Declaration of Competing Interest

The authors declare that they have no known competing financial interests or personal relationships that could have appeared to influence the work reported in this paper.

Acknowledgments

Appendix A. Supplementary data

Supplementary data to this article can be found online at https://doi.org/10.1016/j.compenvurbsys.2022.101890.

References

Acero, J. A., Koh, E. J. Y., Ruefenacht, L. A., & Norford, L. K. (2021). Modelling the influence of high-rise urban geometry on outdoor thermal comfort in Singapore. *Urban Climate, 36*, Article 100775. https://doi.org/10.1016/j.uclim.2021.100775

Adeosun, J. T., & Lawal, A. (2009). Numerical and experimental studies of mixing characteristics in a T-junction microchannel using residence-time distribution. *Chemical Engineering Science, 64*(10), 2422–2432. https://doi.org/10.1016/j.ces.2009.02.013

Alsahli, M. M., & Al-Harbi, M. (2018). Allocating optimum sites for air quality monitoring stations using GIS suitability analysis. *Urban Climate, 24*, 875–886. https://doi.org/10.1016/j.uclim.2017.11.001

An, K., Wong, S.-M. M., & Fung, J. C.-H. H. (2019). Exploration of sustainable building morphologies for effective passive pollutant dispersion within compact urban environments. *Building and Environment, 148*(July 2018), 508–523. https://doi.org/10.1016/j.buildenv.2018.11.030

Antoniou, N., Montazeri, H., Wigo, H., Neophytou, M. K. A. K.-A., Blocken, B., & Sandberg, M. (2017). CFD and wind-tunnel analysis of outdoor ventilation in a real compact heterogeneous urban area: Evaluation using "air delay". *Building and Environment, 126*(October), 355–372. https://doi.org/10.1016/j.buildenv.2017.10.013

Aparicio-Mauricio, G., Rodríguez, F. A., Pijpers, J. J. H., Cruz-Díaz, M. R., & Rivero, E. P. (2020). CFD modeling of residence time distribution and experimental validation in a redox flow battery using free and porous flow. *Journal of Energy Storage, 29*, Article 101337. https://doi.org/10.1016/j.est.2020.101337

Architectural Institute of Japan. (2008). AIJ Guideline for Practical Applications of CFD to Pedestrian Wind Environment around Buildings. Retrieved 16 January 2021, from https://www.aij.or.jp/jpn/publish/cfdguide/index_e.htm.

Architectural Institute of Japan (Ed.). (2016). *AIJ benchmarks for validation of CFD simulations applied to pedestrian wind environment around buildings.* Tokyo: Architectural Institute of Japan.

Azizi, M. M., & Javanmardi, K. (2017). The effects of urban block forms on the patterns of wind and natural ventilation. *Procedia Engineering, 180*, 541–549. https://doi.org/10.1016/j.proeng.2017.04.213

Badach, J., Dymnicka, M., & Baranowski, A. (2020). Urban vegetation in air quality management: A review and policy framework. *Sustainability, 12*(3), 1258. https://doi.org/10.3390/su12031258

Badach, J., Voordeckers, D., Nyka, L., & Van Acker, M. (2020). A framework for air quality management zones - useful GIS-based tool for urban planning: Case studies in Antwerp and Gdańsk. *Building and Environment, 174*, Article 106743. https://doi.org/10.1016/j.buildenv.2020.106743

Barcelo-Ordinas, J. M., Garcia-Vidal, J., Doudou, M., Rodrigo-Munoz, S., & Cerezo-Llavero, A. (2018). Calibrating low-cost air quality sensors using multiple arrays of sensors. In *, Vol. 2018-April. IEEE wireless communications and networking conference, WCNC* (pp. 1–6). https://doi.org/10.1109/WCNC.2018.8377051

Britter, R., & Schatzmann, M. (Eds.). (2007). *Model evaluation guidance and protocol document, COST action 732, quality assurance and improvement of micro-scale meteorological models.* Brussels.

Chang, S., Jiang, Q., & Zhao, Y. (2018). Integrating CFD and GIS into the development of urban ventilation corridors: A case study in Changchun City, China. *Sustainability, 10*(6), 1814. https://doi.org/10.3390/su10061814

Chen, K., Bachmann, P., Bück, A., Jacob, M., & Tsotsas, E. (2019). CFD simulation of particle residence time distribution in industrial scale horizontal fluidized bed. *Powder Technology, 345*, 129–139. https://doi.org/10.1016/j.powtec.2018.12.086

Chen, L., Hang, J., Sandberg, M., Claesson, L., Di Sabatino, S., & Wigo, H. (2017). The impacts of building height variations and building packing densities on flow

adjustment and city breathability in idealized urban models. *Building and Environment, 118*, 344–361. https://doi.org/10.1016/j.buildenv.2017.03.042

Chun, B., & Guldmann, J.-M. (2018). Impact of greening on the urban heat island: Seasonal variations and mitigation strategies. *Computers, Environment and Urban Systems, 71*, 165–176. https://doi.org/10.1016/j.compenvurbsys.2018.05.006

City of London. (2019). Wind microclimate guidelines for developments in the city of London. Retrieved 3 August 2021, from https://www.cityoflondon.gov.uk/service s/planning/microclimate-guidelines.

Ding, C., & Lam, K. P. (2019). Data-driven model for cross ventilation potential in high-density cities based on coupled CFD simulation and machine learning. *Building and Environment, 165*(May), Article 106394. https://doi.org/10.1016/j.buildenv.2019.106394

Dirksen, M., Ronda, R. J., Theeuwes, N. E., & Pagani, G. A. (2019). Sky view factor calculations and its application in urban heat island studies. *Urban Climate, 30*, Article 100498. https://doi.org/10.1016/j.uclim.2019.100498

Du, Y., Blocken, B., & Pirker, S. (2020). A novel approach to simulate pollutant dispersion in the built environment: Transport-based recurrence CFD. *Building and Environment, 170*, Article 106604. https://doi.org/10.1016/j.buildenv.2019.106604

Du, Y., & Mak, C. M. (2018). Improving pedestrian level low wind velocity environment in high-density cities: A general framework and case study. *Sustainable Cities and Society, 42*, 314–324. https://doi.org/10.1016/j.scs.2018.08.001

Duyzer, J., van den Hout, D., Zandveld, P., & van Ratingen, S. (2015). Representativeness of air quality monitoring networks. *Atmospheric Environment, 104*, 88–101. https://doi.org/10.1016/j.atmosenv.2014.12.067

Esri. (2021). ArcGIS Pro geoprocessing tool reference. Retrieved 1 July 2021, from https://pro.arcgis.com/en/pro-app/latest/tool-reference/main/arcgis-pro-tool-re ference.htm.

European Environment Agency (EEA). (2020). Air quality in Europe - 2020 report. EEA Report. Retrieved from https://www.eea.europa.eu/publications/air-quality-in-e urope-2020-report.

Farhadi, H., Faizi, M., & Sanaieian, H. (2019). Mitigating the urban heat island in a residential area in Tehran: Investigating the role of vegetation, materials, and orientation of buildings. *Sustainable Cities and Society, 46*, Article 101448. https://doi.org/10.1016/j.scs.2019.101448

Feng, W., Ding, W., Fei, M., Yang, Y., Zou, W., Wang, L., & Zhen, M. (2020). Effects of traditional block morphology on wind environment at the pedestrian level in cold regions of Xi'an, China. *Environment, Development and Sustainability, 23*(3), 3218–3235. https://doi.org/10.1007/s10668-020-00714-0

Gao, Y., Wang, Z., Liu, C., & Peng, Z.-R. (2019). Assessing neighborhood air pollution exposure and its relationship with the urban form. *Building and Environment, 155*, 15–24. https://doi.org/10.1016/j.buildenv.2018.12.044

Gębicki, J., & Szymańska, K. (2012). Comparative field test for measurement of PM10 dust in atmospheric air using gravimetric (reference) method and β-absorption method (Eberline FH 62-1). *Atmospheric Environment, 54*, 18–24. https://doi.org/10.1016/j.atmosenv.2012.02.068

He, B.-J., Ding, L., & Prasad, D. (2019). Enhancing urban ventilation performance through the development of precinct ventilation zones: A case study based on the greater Sydney, Australia. *Sustainable Cities and Society, 47*, Article 101472. https://doi.org/10.1016/j.scs.2019.101472

He, B.-J., Ding, L., & Prasad, D. (2020). Relationships among local-scale urban morphology, urban ventilation, urban heat island and outdoor thermal comfort under sea breeze influence. *Sustainable Cities and Society, 60*, Article 102289. https://doi.org/10.1016/j.scs.2020.102289

Head Office of Geodesy and Cartography. (2019). General Geographic Database [in Polish]. Retrieved 1 April 2019, from http://www.gugik.gov.pl/strona-glowna.

Henne, S., Brunner, D., Folini, D., Solberg, S., Klausen, J., & Buchmann, B. (2010). Assessment of parameters describing representativeness of air quality in-situ measurement sites. *Atmospheric Chemistry and Physics, 10*(8), 3561–3581. https://doi.org/10.5194/acp-10-3561-2010

Hohenberger, T. L., Che, W., Fung, J. C. H., & Lau, A. K. H. (2021). A proposed population-health based metric for evaluating representativeness of air quality monitoring in cities: Using Hong Kong as a demonstration. *PLoS One, 16*(5), Article e0252290. https://doi.org/10.1371/journal.pone.0252290

Jana, A., Sarkar, A., & Bardhan, R. (2020). Analysing outdoor airflow and pollution as a parameter to assess the compatibility of mass-scale low-cost residential development. *Land Use Policy, 99*, Article 105052. https://doi.org/10.1016/j.landusepol.2020.105052

Janssen, S., Dumont, G., Fierens, F., Deutsch, F., Maiheu, B., Celis, D., & Mensink, C. (2012). Land use to characterize spatial representativeness of air quality monitoring stations and its relevance for model validation. *Atmospheric Environment, 59*, 492–500. https://doi.org/10.1016/j.atmosenv.2012.05.028

Javanroodi, K., Mahdavinejad, M., & Nik, V. M. (2018). Impacts of urban morphology on reducing cooling load and increasing ventilation potential in hot-arid climate. *Applied Energy, 231*(May), 714–746. https://doi.org/10.1016/j.apenergy.2018.09.116

Javanroodi, K., & Nik, V. M. (2020). Interactions between extreme climate and urban morphology: Investigating the evolution of extreme wind speeds from mesoscale to microscale. *Urban Climate, 31*, Article 100544. https://doi.org/10.1016/j.uclim.2019.100544

Jia, B., Liu, S., & Ng, M. (2021). Air quality and key variables in high-density housing. *Sustainability, 13*(8), 4281. https://doi.org/10.3390/su13084281

Johansson, E., & Yahia, M. W. (2020). Wind comfort and solar access in a coastal development in Malmö, Sweden. *Urban Climate, 33*, Article 100645. https://doi.org/10.1016/j.uclim.2020.100645

Juan, Y.-H., Wen, C.-Y., Li, Z., & Yang, A.-S. (2021). A combined framework of integrating optimized half-open spaces into buildings and an application to a

realistic case study on urban ventilation and air pollutant dispersion. *Journal of Building Engineering, 44*, Article 102975. https://doi.org/10.1016/j.jobe.2021.102975

Kaseb, Z., Hafezi, M., Tahbaz, M., & Delfani, S. (2020). A framework for pedestrian-level wind conditions improvement in urban areas: CFD simulation and optimization. *Building and Environment, 184*, Article 107191. https://doi.org/10.1016/j.buildenv.2020.107191

Kurppa, M., Hellsten, A., Auvinen, M., Raasch, S., Vesala, T., & Järvi, L. (2018). Ventilation and air quality in city blocks using large-Eddy simulation—urban planning perspective. *Atmosphere, 9*(2), 65. https://doi.org/10.3390/atmos9020065

Lauriks, T., Longo, R., Baetens, D., Derudi, M., Parente, A., Bellemans, A., & Denys, S. (2021). Application of improved CFD modeling for prediction and mitigation of traffic-related air pollution hotspots in a realistic urban street. *Atmospheric Environment, 246*, Article 118127. https://doi.org/10.1016/j.atmosenv.2020.118127

Li, F., Zhou, T., & Lan, F. (2021). Relationships between urban form and air quality at different spatial scales: A case study from northern China. *Ecological Indicators, 121*, Article 107029. https://doi.org/10.1016/j.ecolind.2020.107029

Li, M., Qiu, X., Shen, J., Xu, J., Feng, B., He, Y., … Zhu, X. (2019). CFD simulation of the wind field in Jinjiang City using a building data generalization method. *Atmosphere, 10*(6). https://doi.org/10.3390/atmos10060326

Li, Z., Zhang, H., Wen, C. Y., Yang, A. S., & Juan, Y. H. (2020). Effects of frontal area density on outdoor thermal comfort and air quality. *Building and Environment, 180*, Article 107028. https://doi.org/10.1016/j.buildenv.2020.107028

Liao, W., Hong, T., & Heo, Y. (2021). The effect of spatial heterogeneity in urban morphology on surface urban heat islands. *Energy and Buildings, 244*, Article 111027. https://doi.org/10.1016/j.enbuild.2021.111027

Lin, M., Hang, J., Li, Y., Luo, Z., & Sandberg, M. (2014). Quantitative ventilation assessments of idealized urban canopy layers with various urban layouts and the same building packing density. *Building and Environment, 79*, 152–167. https://doi.org/10.1016/j.buildenv.2014.05.008

Liu, M., Chen, H., Wei, D., Wu, Y., & Li, C. (2021). Nonlinear relationship between urban form and street-level PM2.5 and CO based on mobile measurements and gradient boosting decision tree models. *Building and Environment, 205*, Article 108265. https://doi.org/10.1016/j.buildenv.2021.108265

Liu, X., Xu, M., Yao, H., Yu, D., Lv, D., & Zhou, K. (2008). The formation and emission of particulate matter during the combustion of density separated coal fractions. *Energy and Fuels, 22*(6), 3844–3851. https://doi.org/10.1021/EF800239V

Łowicki, D. (2019). Landscape pattern as an indicator of urban air pollution of particulate matter in Poland. *Ecological Indicators, 97*, 17–24. https://doi.org/10.1016/j.ecolind.2018.09.050

Lynch, D. H. (2018). AIJ: Case E | Architecture & Construction | SimScale. Retrieved 16 January 2021, from https://www.simscale.com/projects/dlynch/aij_case_e/.

Ma, T., & Chen, T. (2020). Classification and pedestrian-level wind environment assessment among Tianjin's residential area based on numerical simulation. *Urban Climate, 34*, Article 100702. https://doi.org/10.1016/j.uclim.2020.100702

Main Inspectorate of Environmental Protection (GIOŚ) in Poland. (2021). Główny Inspektorat Ochrony Środowiska [Main Inspectorate of Environmental Protection in Poland]. Bank danych pomiarowych [Measurements databank]. https://powietrze.gios.gov.pl/pjp/archives.

Maing, M. (2022). Superblock transformation in Seoul megacity: Effects of block densification on urban ventilation patterns. *Landscape and Urban Planning, 222* (March 2021), 104401. https://doi.org/10.1016/j.landurbplan.2022.104401

Middel, A., Lukaszczyk, J., Maciejewski, R., Demuzere, M., & Roth, M. (2018). Sky view factor footprints for urban climate modeling. *Urban Climate, 25*, 120–134. https://doi.org/10.1016/j.uclim.2018.05.004

Mirzaei, P. A. (2021). CFD modeling of micro and urban climates: Problems to be solved in the new decade. *Sustainable Cities and Society, 69*, Article 102839. https://doi.org/10.1016/j.scs.2021.102839

Mirzaei, P. A., & Haghighat, F. (2012). A procedure to quantify the impact of mitigation techniques on the urban ventilation. *Building and Environment, 47*, 410–420. https://doi.org/10.1016/j.buildenv.2011.06.007

Peng, Y., Gao, Z., Buccolieri, R., & Ding, W. (2019). An investigation of the quantitative correlation between urban morphology parameters and outdoor ventilation efficiency indices. *Atmosphere, 10*(1), 33. https://doi.org/10.3390/atmos10010033

Peng, Y., Gao, Z., Buccolieri, R., Shen, J., & Ding, W. (2021). Urban ventilation of typical residential streets and impact of building form variation. *Sustainable Cities and Society, 67*, Article 102735. https://doi.org/10.1016/j.scs.2021.102735

Piersanti, A., Vitali, L., Righini, G., Cremona, G., & Ciancarella, L. (2015). Spatial representativeness of air quality monitoring stations: A grid model based approach. *Atmospheric Pollution Research, 6*(6), 953–960. https://doi.org/10.1016/j.apr.2015.04.005

Poćwierz, M., & Zielonko-Jung, K. (2021). An analysis of wind conditions at pedestrian level in the selected types of multi-family housing developments. *Environmental Fluid Mechanics, 21*(1), 83–101. https://doi.org/10.1007/s10652-020-09763-5

Qin, H., Lin, P., Lau, S. S. Y., & Song, D. (2020). Influence of site and tower types on urban natural ventilation performance in high-rise high-density urban environment. *Building and Environment, 179*(1239), Article 106960. https://doi.org/10.1016/j.buildenv.2020.106960

Ramponi, R., Blocken, B., de Coo, L. B., & Janssen, W. D. (2015). CFD simulation of outdoor ventilation of generic urban configurations with different urban densities and equal and unequal street widths. *Building and Environment, 92*, 152–166. https://doi.org/10.1016/j.buildenv.2015.04.018

Ren, C., Yang, R., Cheng, C., Xing, P., Fang, X., Zhang, S., & Ng, E. (2018). Creating breathing cities by adopting urban ventilation assessment and wind corridor plan –

The implementation in Chinese cities. *Journal of Wind Engineering and Industrial Aerodynamics, 182*, 170–188. https://doi.org/10.1016/j.jweia.2018.09.023

Righini, G., Cappelletti, A., Ciucci, A., Cremona, G., Piersanti, A., Vitali, L., & Ciancarella, L. (2014). GIS based assessment of the spatial representativeness of air quality monitoring stations using pollutant emissions data. *Atmospheric Environment, 97*, 121–129. https://doi.org/10.1016/j.atmosenv.2014.08.015

Rivas, E., Santiago, J. L., Lechón, Y., Martín, F., Ariño, A., Pons, J. J., & Santamaría, J. M. (2019). CFD modelling of air quality in Pamplona City (Spain): Assessment, stations spatial representativeness and health impacts valuation. *Science of the Total Environment, 649*, 1362–1380. https://doi.org/10.1016/j.scitotenv.2018.08.315

Rodrigues, A. E. (2021). Residence time distribution (RTD) revisited. *Chemical Engineering Science, 230*, Article 116188. https://doi.org/10.1016/J.CES.2020.116188

Rogulski, M., & Badyda, A. (2019). Current trends in network based air quality monitoring systems. *IOP Conference Series: Earth and Environmental Science, 214*, Article 012085. https://doi.org/10.1088/1755-1315/214/1/012085

Santiago, J. L., Rivas, E., Gamarra, A. R., Vivanco, M. G., Buccolieri, R., Martilli, A., … Martín, F. (2022). Estimates of population exposure to atmospheric pollution and health-related externalities in a real city: The impact of spatial resolution on the accuracy of results. *Science of the Total Environment, 819*, Article 152062. https://doi.org/10.1016/j.scitotenv.2021.152062

Santiago, J. L., Martín, F., & Martilli, A. (2013). A computational fluid dynamic modelling approach to assess the representativeness of urban monitoring stations. *Science of the Total Environment, 454–455*, 61–72. https://doi.org/10.1016/j.scitotenv.2013.02.068

Sefair, J. A., Espinosa, M., Behrentz, E., & Medaglia, A. L. (2019). Optimization model for urban air quality policy design: A case study in Latin America. *Computers, Environment and Urban Systems, 78*, Article 101385. https://doi.org/10.1016/j.compenvurbsys.2019.101385

Shi, Y., Ren, C., Lau, K. K. L., & Ng, E. (2019). Investigating the influence of urban land use and landscape pattern on PM2.5 spatial variation using mobile monitoring and WUDAPT. *Landscape and Urban Planning, 189*(November 2018), 15–26. https://doi.org/10.1016/j.landurbplan.2019.04.004

Shi, Y., Xie, X., Fung, J. C. H., & Ng, E. (2018). Identifying critical building morphological design factors of street-level air pollution dispersion in high-density built environment using mobile monitoring. *Building and Environment, 128*, 248–259. https://doi.org/10.1016/j.buildenv.2017.11.043

da Silva, F., Reis, N. C., Santos, J. M., Goulart, E. V., & Engel de Alvarez, C. (2021). The impact of urban block typology on pollutant dispersion. *Journal of Wind Engineering and Industrial Aerodynamics, 210*, Article 104524. https://doi.org/10.1016/j.jweia.2021.104524

da Silva, F. T., Reis, N. C., Santos, J. M., Goulart, E. V., & de Alvarez, C. E. (2022). Influence of urban form on air quality: The combined effect of block typology and urban planning indices on city breathability. *Science of the Total Environment, 814*, Article 152670. https://doi.org/10.1016/j.scitotenv.2021.152670

Solazzo, E., Vardoulakis, S., & Cai, X. (2011). A novel methodology for interpreting air quality measurements from urban streets using CFD modelling. *Atmospheric Environment, 45*(29), 5230–5239. https://doi.org/10.1016/j.atmosenv.2011.05.022

Tian, Y., Yao, X., & Chen, L. (2019). Analysis of spatial and seasonal distributions of air pollutants by incorporating urban morphological characteristics. *Computers, Environment and Urban Systems, 75*, 35–48. https://doi.org/10.1016/j.compenvurbsys.2019.01.003

Van Ryswyk, K., Prince, N., Ahmed, M., Brisson, E., Miller, J. D., & Villeneuve, P. J. (2019). Does urban vegetation reduce temperature and air pollution concentrations? Findings from an environmental monitoring study of the Central Experimental Farm in Ottawa, Canada. *Atmospheric Environment, 218*, Article 116886. https://doi.org/10.1016/j.atmosenv.2019.116886

Voordeckers, D., Lauriks, T., Denys, S., Billen, P., Tytgat, T., & Van Acker, M. (2021). Guidelines for passive control of traffic-related air pollution in street canyons: An overview for urban planning. *Landscape and Urban Planning, 207*, Article 103980. https://doi.org/10.1016/j.landurbplan.2020.103980

Voordeckers, D., Meysman, F. J. R., Billen, P., Tytgat, T., & Van Acker, M. (2021). The impact of street canyon morphology and traffic volume on NO2 values in the street canyons of Antwerp. *Building and Environment, 197*, Article 107825. https://doi.org/10.1016/j.buildenv.2021.107825

Wang, B., Cot, L. D., Adolphe, L., Geoffroy, S., & Sun, S. (2017). Cross indicator analysis between wind energy potential and urban morphology. *Renewable Energy, 113*, 989–1006. https://doi.org/10.1016/j.renene.2017.06.057

Wang, W., Wang, X., & Ng, E. (2021). The coupled effect of mechanical and thermal conditions on pedestrian-level ventilation in high-rise urban scenarios. *Building and Environment, 191*, Article 107586. https://doi.org/10.1016/j.buildenv.2021.107586

Wang, W., Yang, T., Li, Y., Xu, Y., Chang, M., & Wang, X. (2020). Identification of pedestrian-level ventilation corridors in downtown Beijing using large-eddy simulations. *Building and Environment, 182*, Article 107169. https://doi.org/10.1016/j.buildenv.2020.107169

Wang, Z., Calderón, L., Patton, A. P., Sorensen Allacci, M. A., Senick, J., Wener, R., … Mainelis, G. (2016). Comparison of real-time instruments and gravimetric method when measuring particulate matter in a residential building. *Journal of the Air and Waste Management Association, 66*(11), 1109–1120. https://doi.org/10.1080/10962247.2016.1201022

Wojnowski, W., Wei, S., Li, W., Yin, T., Li, X. X., Ow, G. L. F., … Whittle, A. J. (2021). Comparison of absorbed and intercepted fractions of PAR for individual trees based on radiative transfer model simulations. *Remote Sensing, 13*(6). https://doi.org/10.3390/rs13061069

Wong, M. S., Nichol, J. E., To, P. H., & Wang, J. (2010). A simple method for designation of urban ventilation corridors and its application to urban heat island analysis. *Building and Environment, 45*(8), 1880–1889. https://doi.org/10.1016/j.buildenv.2010.02.019

World Health Organization. (2022). Air pollution. Retrieved 30 June 2022, from https://www.who.int/health-topics/air-pollution#tab=tab_1.

Xu, G., Zhou, Z., Jiao, L., & Zhao, R. (2020). Compact urban form and expansion pattern slow down the decline in urban densities: A global perspective. *Land Use Policy, 94*, Article 104563. https://doi.org/10.1016/j.landusepol.2020.104563

Xu, Y., Ren, C., Ma, P., Ho, J., Wang, W., Lau, K. K. L., … Ng, E. (2017). Urban morphology detection and computation for urban climate research. *Landscape and Urban Planning, 167*(July), 212–224. https://doi.org/10.1016/j.landurbplan.2017.06.018

Yang, J., Shi, B., Shi, Y., Marvin, S., Zheng, Y., & Xia, G. (2020). Air pollution dispersal in high density urban areas: Research on the triadic relation of wind, air pollution, and urban form. *Sustainable Cities and Society, 54*, Article 101941. https://doi.org/10.1016/j.scs.2019.101941

Yang, J., Shi, B., Zheng, Y., Shi, Y., & Xia, G. (2020). Urban form and air pollution disperse: Key indexes and mitigation strategies. *Sustainable Cities and Society, 57* (November 2019), 101955. https://doi.org/10.1016/j.scs.2019.101955

Yardeny, I., Portnikov, D., & Kalman, H. (2020). Experimental investigation of the coefficient of restitution of particles colliding with surfaces in air and water. *Advanced Powder Technology, 31*(9), 3747–3759. https://doi.org/10.1016/J.APT.2020.07.018

Yu, B., Liu, H., Wu, J., Hu, Y., & Zhang, L. (2010). Automated derivation of urban building density information using airborne LiDAR data and object-based method. *Landscape and Urban Planning, 98*(3–4), 210–219. https://doi.org/10.1016/j.landurbplan.2010.08.004

Yuan, C., Ng, E., & Norford, L. K. (2014). Improving air quality in high-density cities by understanding the relationship between air pollutant dispersion and urban morphologies. *Building and Environment, 71*, 245–258. https://doi.org/10.1016/j.buildenv.2013.10.008

Yuan, C., Shan, R., Zhang, Y., Li, X.-X., Yin, T., Hang, J., & Norford, L. (2019). Multilayer urban canopy modelling and mapping for traffic pollutant dispersion at high density urban areas. *Science of the Total Environment, 647*, 255–267. https://doi.org/10.1016/j.scitotenv.2018.07.409

Zhang, S., Kwok, K. C. S., Liu, H., Jiang, Y., Dong, K., & Wang, B. (2021). A CFD study of wind assessment in urban topology with complex wind flow. *Sustainable Cities and Society, 71*, Article 103006. https://doi.org/10.1016/j.scs.2021.103006